

CRADMap: Applied Distributed Volumetric Mapping with 5G-Connected Multi-Robots and 4D Radar Sensing

Maaz Qureshi¹, Alexander Werner¹, Zhenan Liu¹, Amir Khajepour¹, George Shaker¹, and William Melek¹

Abstract—Sparse and feature SLAM methods provide robust camera pose estimation. However, they often fail to capture the level of detail required for inspection and scene awareness tasks. Conversely, dense SLAM approaches generate richer scene reconstructions but impose a prohibitive computational load to create 3D maps. We present a novel distributed volumetric mapping framework designated as CRADMap that addresses these issues by extending the state-of-the-art (SOTA) ORBSLAM3 [1] system with the COVINS [2] on the backend for global optimization. Our pipeline for volumetric reconstruction fuses dense keyframes at a centralized server via 5G connectivity, aggregating geometry, and occupancy information from multiple autonomous mobile robots (AMRs) without overtaxing onboard resources. This enables each AMR to independently perform mapping while the backend constructs high-fidelity 3D maps in real time. To overcome the limitation of standard visual nodes we automate a 4D mmWave radar, standalone from CRADMap, to test its capabilities for making extra maps of the hidden metallic object(s) in a cluttered environment. Experimental results Section-IV confirm that our framework yields globally consistent volumetric reconstructions and seamlessly supports applied distributed mapping in complex indoor environments. -*GitHub Repository*: <http://surl.li/xgfpdx>

I. INTRODUCTION

The rapid development of robot autonomy has opened up new opportunities to automate routine tasks and improve safety in hazardous environments. With reliable simultaneous localization and mapping (SLAM) systems robust in pose estimation and map generation, there is a growing gap in multi-robot distributed SLAM to build detailed 3D maps using low-cost autonomous mobile robots (AMRs), with limited processing capabilities, for real-time and efficient mapping. Such systems are essential for applications such as navigation, path planning, and inspection. Mapping large complex indoor environments presents several unresolved problems. First, coordinating data from multiple robots to generate a dense, volumetric map requires significant computational power. Second, handling overlapping sensor data from multiple AMRs while maintaining distributed maps accuracy remains a critical issue. Third, although high-speed data transmission from WiFi offers great potential, managing high bandwidth with low latency for real-time performance is not trivial.

Industries such as manufacturing, warehouse management, and asset or infrastructure inspection, which rely on autonomous robotics in damage monitoring, digital inspections,

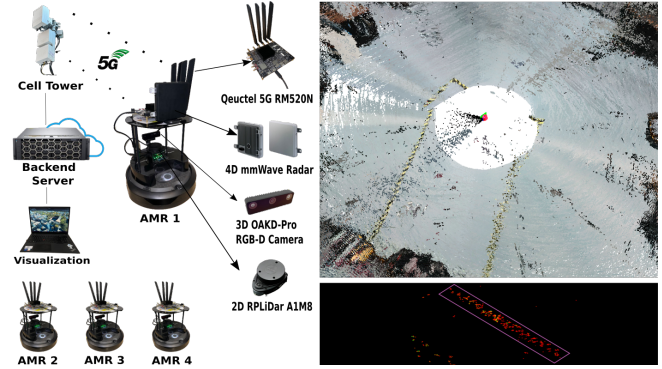


Fig. 1. An overview of our approach on the left shows the data transmission cycle for map visualization. The center highlights an AMR [3] with key components integrated. The right side shows the top-view 360-degree CRADMap of UW RoboHub lab, while the bottom right displays the radar point cloud map detecting obscured vent pipe.

and material handling, require the deployment of reliable solutions to enable the efficient completion of the aforementioned tasks. These environments are large and often cluttered with obstacles like machinery, walls, and structural elements, which can obstruct the view of visual sensors. This limitation affects tasks that require precise navigation and detailed mapping with a team of AMRs. As industrial applications become more demanding, there is a growing need for systems that can effectively manage these complexities and deliver reliable real-time mapping.

In response to these challenges we develop CRADMap, a novel scalable distributed volumetric mapping architecture that utilize ORBSLAM3 on the frontend [1] with the COVINS [2] on the backend, an overview shown in Figure. 1. In our approach, we enhance keyframes so that they not only store the camera pose (i.e., its position and orientation) and visual features but also include a complete 3D dense point cloud. This enriched data is transmitted over 5G to achieve high bandwidth with low latency to the backend server, which fuses keyframes from view, integrates dense point clouds, and reconstructs the scene to generate globally consistent, high-fidelity 3D maps in real-time. Additionally, since visual nodes miss objects hidden by obstacles, we automated an independent 4D mmWave radar that creates its point map to detect occluded or hidden metallic objects.

The main contributions of this work are as follows:

- Mapping framework (CRADMap) that enhances Visual-SLAM with enriched keyframes containing dense point clouds to generate volumetric maps in real-time.
- A multi-robot distributed architecture that leverages a

*This work is supported by Rogers Communication Inc and Mitacs.

¹All authors are with the Faculty of Mechanical and Mechatronics Engineering, University of Waterloo (UW), 200 University Ave W, Waterloo, ON N2L3G1, Canada. Corresponding Author Email: m23qures@uwaterloo.ca

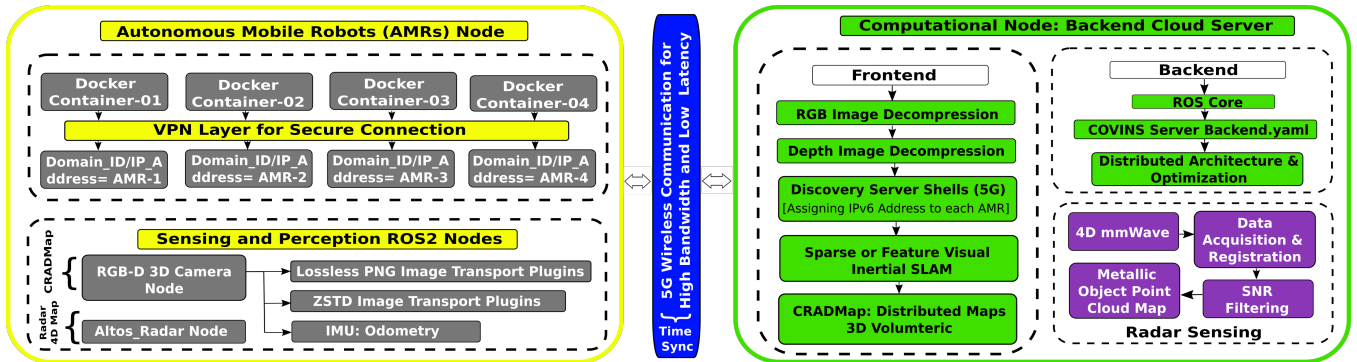


Fig. 2. The comprehensive process flow of methodology. The yellow box illustrates the structure of the AMRs ROS2 nodes along with the sensing suites. The green box represents the frontend and backend stages corresponding to the distributed framework for multi-robot volumetric map and radar point cloud maps, managed on a central server to offload computational processing, while the middle stage in the blue channel for real-time data transmission.

high-bandwidth i.e. 5G network to offload intensive processing to a centralized COVINS backend, ensuring real-time, globally optimized 3D reconstructions.

- Integration of an independent 4D mmWave radar that creates a standalone point cloud map, supplementing visual data to improve the detection of hidden structures in complex indoor settings.
- Evaluation of live experiments from multiple AMRs to demonstrate mapping improvements 5G efficiency.

The paper is organized as follows. Section II discusses related work, and Section III describes the overall system methods. Experiments are presented in Section IV. Lastly, Section V presents the conclusion with future work.

II. RELATED WORK

A. Volumetric mapping

Early RGB-D SLAM efforts by Henry et al. [4] and Endres et al. [5] achieved dense reconstructions yet often relied on offline optimization and high-end GPUs, making them impractical for real-time volumetric mapping. KinectFusion [6] introduced TSDF-based mapping for smaller indoor spaces, leveraging powerful hardware to sustain real-time performance. Later works such as voxel hashing by Nießner et al. [7] scaled KinectFusion to larger scenes, while Oleynikova et al. [8] (Voxblox) and Millane et al. [9] (Voxgraph) refined incremental fusion and drift correction mainly in single-AMR or offline settings. Additionally, an octree-based approach by Hou et al. [10] processed RGB-D video for real-time 3D indoor mapping, but it remained limited to a single-AMR pipeline without addressing the complexity of multi-robot collaboration. As a result, large-scale 3D volumetric maps on low-cost AMRs remain a key challenge, especially under live conditions.

B. Multi-Robots SLAM Techniques and 5G Communication

Modern distributed and decentralized SLAM solutions such as Kimera-Multi [11] and Swarm-SLAM [12] extend multi-robot mappings frameworks advance multi-agent coordination but demand significant GPU resources on limited bandwidth networks. Meanwhile, CCM-SLAM [13] and COVINS [2] reduce global drift by merging keyframes

on a centralized backend server, primarily handling sparse data. Our approach extends ORBSLAM3 [1] with COVINS [2], showing that centralized global optimization enhances keyframe accuracy for multi-robot in distributed architecture instead of map merging. To handle dense volumetric data from multiple robots in real-time, we utilize 5G communication, as highlighted by recent work [14] demonstrating how high throughput and low latency enable offloading of large sensor streams. By transmitting dense keyframes over 5G, our system alleviates each AMR computing load, allowing real-time distributed volumetric reconstruction.

C. 4D mmWave Sensing Technology

Although radar-based SLAM [15], [16] can improve navigation in harsh visibility i.e. fog, snow, and low lighting, it introduces complex sensor fusion, and potential noise not present in indoor environments. Motivated from Doojin Lee et al [17] and Wallabot [18] illustrate the radar unique capability for detecting metallic or hidden objects behind walls. In our framework, radar operates separately from the CRADMap pipeline, focusing on detecting obscured objects that are not visible by camera or lidar. This modular design maintains a streamlined volumetric map referred to here as CRADMap and in addition, delivers a standalone radar point cloud map for detecting metal items that are obscured behind furniture and walls.

III. METHODS

Our proposed system, CRADMap, is a distributed multi-robot framework for applied volumetric mapping that uses ORBSLAM3 [1] on front-ends, a centralized COVINS [2] on back-end for distributed architecture, and a dedicated Altos 4D mmWave radar [20] to generate additional point cloud map of obscured metallic object(s). Fig. 2 illustrates the detailed process blocks involved. The system leverages high-bandwidth 5G connectivity (≈ 24 ms end-to-end latency, up to 110 MBps) to enable four AMRs (autonomous mobile robots) as shown in Fig. 1. Each integrated with quectel 5G RM520N [21] to stream data in real-time with OAK-D pro [22] 3D RBG-D camera, with inherent scalability to N AMRs. In the following, we describe our research

TABLE I
5G NR FREQUENCY BAND PARAMETERS [19] FOR TIME DIVISION DUPLEXING (TDD) COMMUNICATION

Band	Name	Mode	Δ FRaster (kHz)	Low (MHz)	Middle (MHz)	High (MHz)	DL/UL Bandwidth (MHz)
78	TD 3500	TDD	15, 30	3300	3550	3800	500

pipeline supported by algorithms to illustrate the flow of implementation.

A. Front-End: ORBSLAM3 with Dense Keyframe Generation

Each AMR processes an RGB-D data stream (I_t, D_t) at time t using ORBSLAM3 to extract features and estimate camera poses. Our method enriches standard ORBSLAM3 keyframes by generating dense point clouds, which facilitate robust volumetric mapping.

i. Feature Extraction and Pose Estimation

a) *ORB Feature Extraction*: For each frame I_t , ORBSLAM3 extracts 2D keypoints $\{f_{ij}\}$ (with i indexing keyframes and j indexing keypoints).

b) *Depth Association*: For each detected keypoint at pixel u_{ij} , the depth d_{ij} is retrieved from the depth image D_t . The corresponding 3D point x_{ij} is computed via:

$$x_{ij} = \Pi^{-1}(u_{ij}, d_{ij}) = d_{ij} \cdot K^{-1} \begin{bmatrix} u_{ij} \\ 1 \end{bmatrix} \quad (1)$$

where Π^{-1} is the back-projection operator using camera intrinsics (K).

c) *Pose Estimation*: The camera pose $T_t \in SE(3)$ is obtained by minimizing the reprojection error:

$$T_t = \arg \min_{T \in SE(3)} \sum_{i,j} \|u_{ij} - \pi(T \cdot x_{ij})\|^2 \quad (2)$$

Here, $\pi(\cdot)$ projects a 3D point onto the image plane, ensuring alignment between observed key points and reprojected 3D points. $SE(3)$ is a special Euclidean group in three dimensions.

ii. Dense Keyframe Generation

d) *Dense Point Cloud Construction*: When keyframe criteria (e.g., significant camera motion or scene change) are met, a dense point cloud is generated from the entire image:

$$P_i = \{x \mid x = \Pi^{-1}(u, D_i[u]), u \in \Omega(I_i)\} \quad (3)$$

where $\Omega(I_i)$ is the set of all pixel coordinates in image I_i .

e) *Outlier Removal*: To improve robustness, we filter out noisy points by comparing each point x to the local neighborhood statistics:

$$\|x - \mu_N(x)\| \leq \lambda \sigma_N(x) \quad (4)$$

where $\mu_N(x)$ and $\sigma_N(x)$ are the mean and standard deviation of neighboring points, and λ is a threshold. The cleaned point cloud is denoted as P_i^{clean} .

f) *Keyframe Packaging*: The keyframe is then stored as:

$$K_i = \{T_i, \{f_{ij}\}, I_i, D_i, P_i^{\text{clean}}\} \quad (5)$$

which includes the estimated pose T_i , features, RGB-D images, and the cleaned dense point cloud.

iii. Image Plugins and 5G Bandwidth

For real-time streaming we use lossless PNG compression for RGB (15 FPS) and ZSTD for depth (10 FPS) ROS2 camera topics using image transport plugins [23]. Compressed images are sent to the cloud backend server for pose optimization and distributed map handling in COVINS. This integration ensures the creation of accurate dense volumetric maps. Each AMR is assigned a unique IPv6 address via the 5G Wwan, enabling real-time streaming and SLAM processing. We operate in the NR FR1 channel details presented in Table I which supports high data rates required for RGB-D cameras. The 5G network ensures fast IPv6-based discovery and low latency for experiments.

g) *Bandwidth Calculation*: each-AMR bandwidth (B_r)

$$B_r = f \times (PNG_{\text{comp}}^{\text{RGB}} + ZSTD_{\text{comp}}^{\text{depth}}) \quad (6)$$

Total bandwidth for four AMRs:

$$B_{\text{total}} = \sum_{r=1}^4 B_r \leq 110 \text{ Mbps} \quad (7)$$

Algorithm 1 Dense Keyframe Generation

Require: RGB-D stream (I_t, D_t) for each frame t

Ensure: Stream of keyframes $\{K_i\}$

```

1: for each frame  $t$  do
2:   Feature Extraction & Depth Association:
3:   Detect ORB keypoints in  $I_t$ 
4:   for each detected keypoint  $u_{ij}$  do
5:     Retrieve depth  $d_{ij}$  from  $D_t$ 
6:     Compute 3D point  $x_{ij}$  (Eq. 1)
7:   end for
8:   Pose Estimation:
9:   Estimate  $T_t$  by minimizing error (Eq. 2)
10:  Keyframe Decision & Generation
11:  if keyframe criteria are met then
12:    Generate dense  $P_i$  from  $I_t$  and  $D_t$  (Eq. 3)
13:    Filter  $P_i$  to obtain  $P_i^{\text{clean}}$  (Eq. 4)
14:    Package keyframe  $K_i$  (Eq. 5)
15:    Compress  $I_t$  (PNG) and  $D_t$  (zstd) (Eqs. 6)
16:    Transmit  $K_i$  over the 5G network (Eqs. 7)
17:  end if
18: end for
19: return  $\{K_i\}$ 

```

B. Back-End: COVINS for Optimizations

The COVINS back-end receives keyframes from all AMRs, stores them in a global Atlas, and performs loop closure and pose graph optimization to refine camera poses and reduce drift. COVINS improves Absolute Trajectory Error (ATE) and Root Mean Square Error (RMSE) through global

consistency and loop closure, it maintain the individual maps from each AMR (RGB-D) in a distributed manner instead of collaborative map merging.

i. Keyframe Integration

a) Keyframes (K_i) are stored in the atlas as:

$$K_i = \{T_i, P_i^{\text{clean}}, \{f_{ij}\}\} \quad (8)$$

ii. Loop Closure and Global Pose Optimization

b) *Loop Closure Constraint*: For a new keyframe K_n , candidate keyframes K_j are identified via a Bag-of-Words approach. A loop closure constraint is computed as:

$$C(T_n, T_j) = T_n^{-1} T_j \quad (9)$$

c) *Global Pose Optimization*: The global pose graph is refined by minimizing a cost function that combines odometry and loop closure constraints:

$$\{T_i^*\} = \arg \min_{\{T_i\}} \left(\sum_{(i,k) \in E_{\text{odom}}} \|\Delta(T_i, T_k)\|_{\Sigma_{\text{odom}}}^2 + \sum_{(i,k) \in E_{\text{loop}}} \|C(T_i, T_k)\|_{\Sigma_{\text{loop}}}^2 \right) \quad (10)$$

Here, $\Delta(T_i, T_k)$ represents the relative odometry error, and Σ_{odom} and Σ_{loop} are covariance matrices for odometry and loop closure constraints, respectively.

Algorithm 2 COVINS: Pose Optimization and Loop Closure

Require: Set of keyframes $\{K_i\}$ from all AMRs

Ensure: Refined global pose graph $\{T_i^*\}$

- 1: Keyframe Integration:
 - 2: **for** each incoming keyframe K_i **do**
 - 3: Store K_i in the global atlas
 - 4: **end for**
 - 5: Loop Closure Detection:
 - 6: **for** each new keyframe K_n **do**
 - 7: Identify candidate keyframes using Bag-of-Words
 - 8: **for** each candidate K_j **do**
 - 9: Compute loop closure constraint (Eq. 9)
 - 10: **end for**
 - 11: **end for**
 - 12: Global Optimization: Optimize global pose graph by minimizing combined cost function (Eq. 10)
 - 13: Update & Broadcast: Refined poses $\{T_i^*\}$ to all AMRs
 - 14: Update global atlas
 - 15: **return** $\{T_i^*\}$
-

C. Distributed Volumetric Mapping

In CRADMap, each AMR constructs its individual volumetric map from dense keyframes, transformed into the global coordinate frame using refined poses from COVINS. The distributed framework operates as follows: each AMR independently processes its RGB-D stream, generates dense keyframes from frontend (III-A), and builds a local map without map merging in a distributed manner (III-B). This

pipeline ensures scalability by eliminating the need for computationally expensive map merging, and robustness against individual AMR failures. Each AMR r generates a local map M_r by transforming the dense point clouds from each keyframe into the global coordinate frame using the refined pose:

$$X = T_i^* \cdot x, \forall x \in P_i \quad (11)$$

Then, the local map is formed as the union of all transformed points:

$$M_r(\text{CRADMap}) = \bigcup_{i \in K_r} \{X\} \quad (12)$$

4D Radar-Metallic Object Detection

4D mmWave radar enable the detection of hidden metallic structures automatically triggers where camera fail. Weighting point cloud registration with SNR data filters outliers and filtering non-metallic returns, enhancing metallic detection for mapping hidden utilities as shown in section IV-D.

i. *Radar Data Acquisition and SNR Filtering*: At time t , the radar produces a point cloud $R_t = \{r_k\}$. Points are filtered based on SNR:

$$R_t^{\text{metal}} = \{r_k \in R_t \mid s_k \geq s_{\text{th}}\} \quad (13)$$

ii. *Global Transformation and Noise Removal*: Filtered radar points are transformed to the global frame:

$$Z = T_i^* \cdot r_k \cdot \begin{bmatrix} \cos \theta_k \cos \phi_k \\ \sin \theta_k \cos \phi_k \\ \sin \phi_k \end{bmatrix} \quad (14)$$

A statistical outlier removal filter is then applied to Z :

$$M_{\text{radar}} = \{Z \mid Z \text{ passes noise filtering}\} \quad (15)$$

Algorithm 3 4D Radar: Metallic Object Detection

Require: Radar point cloud R_t with measurements $(r_k, \theta_k, \phi_k, d_k, s_k)$ at time t

Ensure: Metallic detection map M_{radar}

- 1: **Radar Triggering:**
 - 2: **if** Camera detects: Wall || occlusion (furniture) **then**
 - 3: Activate radar
 - 4: **else**
 - 5: **return** (Exit if no occlusion or wall)
 - 6: **end if**
 - 7: **SNR Filtering:**
 - 8: **for** each radar measurement in R_t **do**
 - 9: **if** $s_k \geq s_{\text{th}}$ **then**
 - 10: Retain measurement r_k
 - 11: **end if**
 - 12: **end for**
 - 13: Let R_t^{metal} be retained measurements (Eq. 13)
 - 14: **Global Transformation:**
 - 15: **for** each measurement in R_t^{metal} **do**
 - 16: Transform to global frame (Eq. 14)
 - 17: **end for**
 - 18: **Noise Removal:** Outlier removal get M_{radar} (Eq. 15)
 - 19: **return** M_{radar} (**Radar Point Cloud Map**)
-

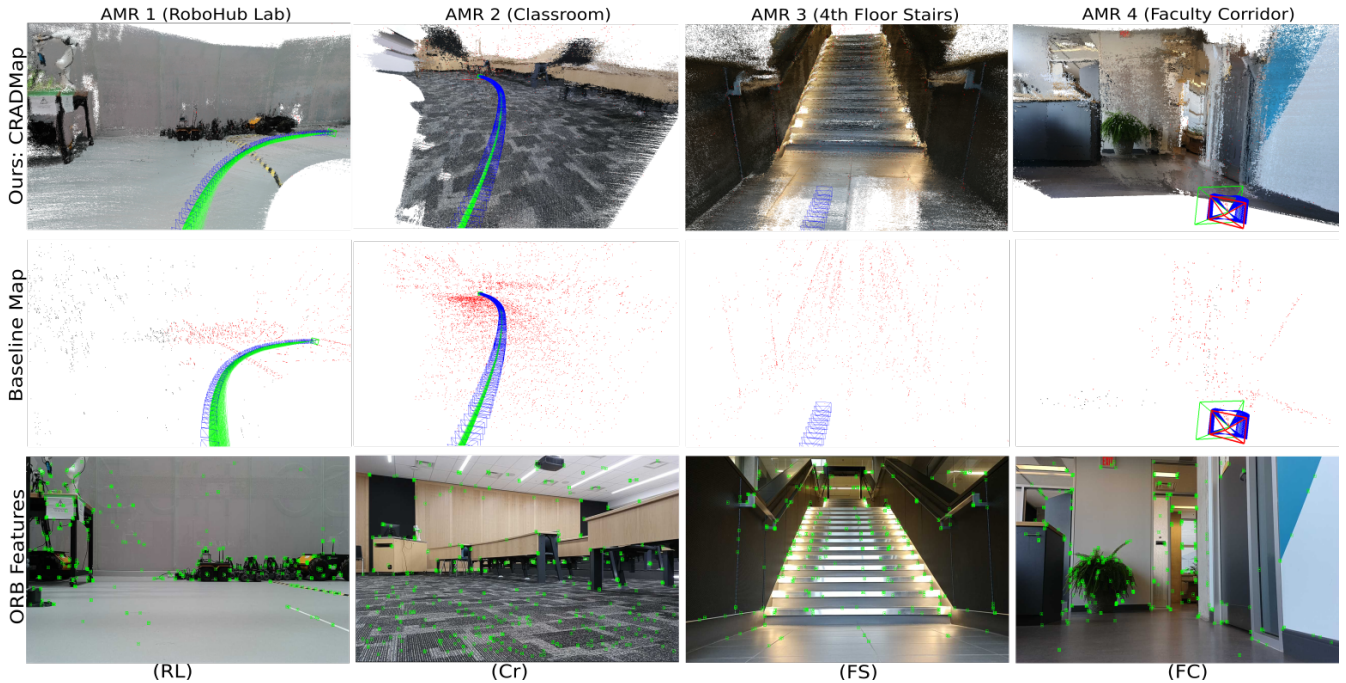


Fig. 3. Qualitative comparison of our dense volumetric map approach (top-row) with the baseline ORBSLAM3 [1], sparse map, (middle-row). The bottom row shows the field of view and orb features detection by frontend SLAM. The dataset is live-captured at different floors of the UW Engineering (UW-E7) building to perform the evaluation.

IV. EXPERIMENT

A. Evaluation Metrics and Dataset

We evaluate our system on the indoor settings (1) live experiments from the University of Waterloo (UW) E7 building and (2) TUM RGB-D benchmark [24]. In UW-E7 we captured 4 scenes as shown in Fig. 3 using four AMRs. All experiments are conducted on hardware Intel i7-1355U, 32GB RAM, Graphics (RPL-U), and software Ubuntu 22.04, ROS2 Humble, with ORBSLAM3 [1] as our baseline. Volumetric mapping quality, CRADMap, and network performance are assessed on the UW-E7 dataset in Open3D [25] on campus Wifi eduroam [26] and 5G network provided by our industry partner, Rogers Inc [27]. 4D mmWave radar detection are evaluate by doing two complex experiments in UW-E7 shown in Fig. 4 and Fig. 5 where partial and complete block view. Lastly, pose estimation metrics performed on a public dataset.

B. CRADMap Evaluation

We generated four distributed dense volumetric maps on live UW-E7 experiments (Robohub Lab, Classroom, Stairs, and Faculty Corridor) using our CRADMap approach. To evaluate mapping, the qualitative comparison is shown in Fig. 3 also we use Open3D for quantitative evaluation to compute coverage (the percentage of the environment reconstructed via a voxel grid over the explored area) and density (points per cubic meter). First, the baseline ORBSLAM3 and our CRADMap are generated to ensure both are in the same coordinate frame, making our relative metrics robust. For example, in the Robohub Lab, glass surfaces cause ORB-SLAM3 to achieve only about 26.91% coverage, while our method reconstructs approximately 78.93%

of the environment with significantly higher point density as shown in Table II. Similarly, in the Classroom, Stairs, and Faculty Corridor, our method consistently yields higher coverage and denser reconstructions than the baseline. These relative improvements in coverage 78% to 85% and $4.6\text{--}5.5\times$ more density provide compelling evidence of our system’s enhanced mapping capabilities.

TABLE II
CRADMAP VOLUMETRIC MAPPING QUALITY QUANTITATIVE ANALYSIS ON UW-E7 EXPERIMENTS

Scene	Coverage (%)		Density (pts/m ³)	
	Baseline	Ours	Baseline	Ours
Robohub Lab	26.91	78.93	161	950
Classroom	37.26	82.82	147	896
Stairs	26.69	85.17	123	782
Faculty Corridor	24.54	79.34	182	1023

C. Network Performance Evaluation

Evaluation perform on live UW-E7 dataset in a multi-robot setup, where each AMR generates visual data at 14 MB/s (112 Mbps) from its RGB (15 Hz) and depth (10Hz) streams. The WiFi network at the UW employs IEEE 802.1X for authentication and both dual-band 2.4 GHz/5 GHz frequency bands. For the evaluation, the 5 GHz and WiFi band are utilized, a single AMR achieves an effective maximum upload speed of 90 Mbps, resulting in an update frequency of approximately 8.9 Hz; however, with 4 AMRs the total load reaches 56MB/s (448 Mbps), and the effective per AMR bandwidth drops to about 22.5 Mbps, which get reduced to around 3.5 Hz using 4 AMRs together. In contrast,

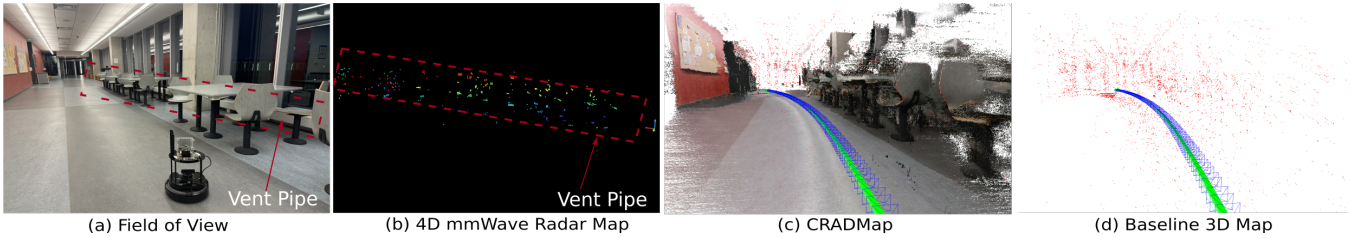


Fig. 4. Cluttered indoor setting with furniture and vent pipe present horizontal with the floor. Only 4D mmWave radar detects successfully in (b).

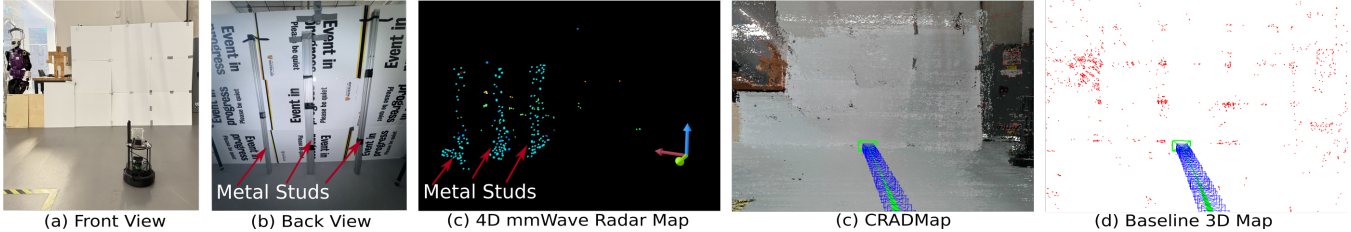


Fig. 5. In complete blocked view 4D mmWave radar sensing shows points cloud map of 3 metal studs behind the hand crafted-wall in (c).

5G (3.5 GHz band, 110 to 120 Mbps upload) maintains a stable latency of 24 ms; with 1 AMR, the update frequency is about 10.4 Hz, and with 4 AMRs, it drops to 7.1 Hz due to shared bandwidth as shown in Table III. These calculations, based on the formula $\text{Map Update Frequency} = (\text{Effective Upload Speed per AMR}) / (\text{Data per Update})$, clearly show that 5G’s higher available bandwidth and stable latency yield significantly better and more predictable performance compared to WiFi.

TABLE III
NETWORK PERFORMANCE QUANTITATIVE COMPARISON ON UW-E7
EXPERIMENTS

Network	Data Rate (MB/s)		Performance	
	AMRs	Total	Latency (ms)	Map (Hz)
WiFi	1	14	8–33 (variable)	8.9
	4	56	11–34 (variable)	3.5
5G	1	14	24 ± 2	10.4
	4	56	24 ± 4	7.1

D. Radar-Enhanced Occluded Object Detection

Behind-the-wall object detection enhance perception beyond visual occlusions [17]. To leverage this capability, we integrate camera-driven situational awareness to dynamically activate radar when a wall or occlusion region is detected using our Algorithm 3, ensuring efficient and targeted sensing. We evaluate 4D mmWave radar capabilities using a 4-chip cascaded imaging radar operating at 77 GHz, which produces high-density point clouds with an angular resolution of 1.4 degrees in both azimuth and elevation. In the (1) scenario, an AMR maps a cluttered indoor aisle at UW-E7, as shown in Fig. 4, where the presence of furniture caused the CRADMap in Fig. 4(c) and baseline map in Fig. 4(d) to miss detecting a horizontal metal ventilation pipe. Missing such structural

components can be dangerous, particularly for AMRs navigating environments, as undetected obstacles may cause collisions. The radar achieved a $92\% \pm 3$ detection rate for the pipe despite some residual noise. Another (2) scenario from Fig. 5(a,b), 3 cm thick, solid opaque wall made of plastic boards are used to completely block the view. Visibility beyond barriers is critical in scenarios such as search-and-rescue operations, and construction site inspections. Ground truth are establish via manual annotation placing marker points on the metal studs behind the wall and vent pipe as well, and after filtering out noise and non-metallic reflections, the radar system accurately detected all three metal studs, achieving a $84\% \pm 5$ detection rate. These results demonstrate that radar integration significantly enhances obscured object detection in environments where traditional visual nodes i.e. camera and lidar fail.

E. Pose Estimation Evaluation

Our primary goal is to perform volumetric mapping not improving the pose estimation but we evaluate on four TUM RGB-D sequences (fr1/plant, fr1/teddy, fr2/coke, fr2/dishes) in Table IV to validate consistency. We computed ATE and RMSE by averaging results over five runs using the available ground truth. Our method slightly improves ATE and RMSE compared to baseline because the COVINS backend enables global pose-graph optimization, aggregating loop closures to correct drift across the entire trajectory. Dense depth priors from volumetric fusion strengthen bundle adjustment in texture-less regions (e.g., walls, glass), where ORBSLAM3 sparse features struggles, leading to reduced feature matching in low-texture and reflective scenes. However, global pose-graph optimization and loop closures in the COVINS backend help mitigate drift in such scenarios.

TABLE IV
TRAJECTORY ACCURACY ON TUM RGB-D SEQUENCES

Sequence	Metric	ORBSLAM3 (m) $\pm \sigma$	Ours (m) $\pm \sigma$
fr1/plant	ATE	0.1178 \pm 0.0049	0.1043 \pm 0.0045
	RMSE	0.1323 \pm 0.0052	0.1187 \pm 0.0050
fr1/teddy	ATE	0.1432 \pm 0.0051	0.1275 \pm 0.0048
	RMSE	0.1654 \pm 0.0060	0.1482 \pm 0.0057
fr1/coke	ATE	0.1012 \pm 0.0043	0.0905 \pm 0.0039
	RMSE	0.1135 \pm 0.0048	0.1116 \pm 0.0044
fr1/dishes	ATE	0.1476 \pm 0.0059	0.1398 \pm 0.0054
	RMSE	0.1627 \pm 0.0061	0.1635 \pm 0.0056

V. CONCLUSIONS

This work introduced CRADMap, a distributed volumetric mapping framework that bridges sparse and dense SLAM approaches for distributed multi-robot systems and detection in obscured environment. By enhancing ORBSLAM3 [1] with dense keyframes and leveraging COVINS [2] for backend optimization via 5G connectivity, CRADMap achieves globally consistent 3D reconstructions while offloading computational demands. The use of 5G ensures low-latency and high-bandwidth communication, enabling real-time data transmission and 2x faster map update. Experiments demonstrate significant improvements, with 75% to 85% environmental coverage and 4.6x to 5.5x higher point density compared to baseline. The automation of standalone 4D mmWave radar enables the detection of occluded metallic structures, validated in cluttered scenarios achieving detection rates of 84% to 92% where camera alone fail. Future work will investigate the scalability of mmWave 5G in larger environments and expand testing to outdoor scenarios. The primary limitation in our current evaluation is that it relies on relative comparisons with a baseline map, due to the absence of an external laser scanner.

REFERENCES

- [1] C. Campos, R. Elvira, J. J. G. Rodríguez, J. M. Montiel, and J. D. Tardós, “Orb-slam3: An accurate open-source library for visual, visual-inertial, and multimap slam,” *IEEE Transactions on Robotics*, vol. 37, no. 6, pp. 1874–1890, 2021.
- [2] P. Schmuck, T. Ziegler, M. Karrer, J. Perraudin, and M. Chli, “Covins: Visual-inertial slam for centralized collaboration,” in *2021 IEEE International Symposium on Mixed and Augmented Reality Adjunct (ISMAR-Adjunct)*, pp. 171–176, IEEE, 2021.
- [3] “Turtlebot 4: Next-generation mobile robot for ros research and development.” <https://clearpathrobotics.com/turtlebot-4/>. Accessed: 2024-09-12.
- [4] P. Henry, M. Krainin, E. Herbst, X. Ren, and D. Fox, *RGB-D Mapping: Using Depth Cameras for Dense 3D Modeling of Indoor Environments*, pp. 477–491. Berlin, Heidelberg: Springer Berlin Heidelberg, 2014.
- [5] F. Endres, J. Hess, N. Engelhard, J. Sturm, D. Cremers, and W. Burgard, “An evaluation of the rgb-d slam system,” *Proceedings - IEEE International Conference on Robotics and Automation*, pp. 1691–1696, 05 2012.
- [6] R. A. Newcombe, S. Izadi, O. Hilliges, D. Molyneaux, D. Kim, A. J. Davison, P. Kohi, J. Shotton, S. Hodges, and A. Fitzgibbon, “Kinectfusion: Real-time dense surface mapping and tracking,” in *2011 10th IEEE International Symposium on Mixed and Augmented Reality*, pp. 127–136, 2011.
- [7] M. Nießner, M. Zollhöfer, S. Izadi, and M. Stamminger, “Real-time 3d reconstruction at scale using voxel hashing,” *ACM Transactions on Graphics (TOG)*, vol. 32, pp. 1 – 11, 2013.

- [8] H. Oleynikova, Z. Taylor, M. Fehr, R. Siegwart, and J. Nieto, “Voxblox: Incremental 3d euclidean signed distance fields for on-board mav planning,” in *2017 IEEE/RSJ International Conference on Intelligent Robots and Systems (IROS)*, pp. 1366–1373, 2017.
- [9] V. Reijngart, A. Millane, H. Oleynikova, R. Siegwart, C. Cadena, and J. Nieto, “Voxgraph: Globally consistent, volumetric mapping using signed distance function submaps,” *IEEE Robotics and Automation Letters*, vol. 5, no. 1, pp. 227–234, 2020.
- [10] J. Hou, M. Goebel, P. Hübner, and D. Iwaszczuk, “Octree-based approach for real-time 3d indoor mapping using rgb-d video data,” *The International Archives of the Photogrammetry, Remote Sensing and Spatial Information Sciences*, vol. 48, pp. 183–190, 2023.
- [11] Y. Tian, Y. Chang, F. Herrera Arias, C. Nieto-Granda, J. P. How, and L. Carlone, “Kimera-multi: Robust, distributed, dense metric-semantic slam for multi-robot systems,” *IEEE Transactions on Robotics*, vol. 38, no. 4, pp. 2022–2038, 2022.
- [12] P.-Y. Lajoie and G. Beltrame, “Swarm-slam: Sparse decentralized collaborative simultaneous localization and mapping framework for multi-robot systems,” *IEEE Robotics and Automation Letters*, vol. 9, no. 1, pp. 475–482, 2024.
- [13] P. Schmuck and M. Chli, “Ccm-slam: Robust and efficient centralized collaborative monocular simultaneous localization and mapping for robotic teams,” *Journal of Field Robotics*, vol. 36, no. 4, pp. 763–781, 2019.
- [14] K. Komatsu, P. Alavesá, A. Pauanne, T. Hänninen, O. Liinamaa, and A. Pouutu, “Leveraging 5g in cyber-physical system for low-cost robotic telepresence,” in *2022 Joint European Conference on Networks and Communications & 6G Summit (EuCNC/6G Summit)*, pp. 399–404, IEEE, 2022.
- [15] H. A. G. C. Premachandra, R. Liu, C. Yuen, and U.-X. Tan, “Uwb radar slam: An anchorless approach in vision denied indoor environments,” *IEEE Robotics and Automation Letters*, vol. 8, no. 9, pp. 5299–5306, 2023.
- [16] J. Zhang, H. Zhuge, Z. Wu, G. Peng, M. Wen, Y. Liu, and D. Wang, “4dradar slam: A 4d imaging radar slam system for large-scale environments based on pose graph optimization,” in *2023 IEEE International Conference on Robotics and Automation (ICRA)*, pp. 8333–8340, 2023.
- [17] D. Lee, G. Shaker, and W. Melek, “Imaging of human walking behind the obstacle utilizing pulsed radar technique in the c-band for military surveillance applications,” *Journal of Electrical Engineering & Technology*, vol. 15, no. 3, pp. 1431–1439, 2020.
- [18] “Walabot 3d imaging sensor technology.” <https://walabot.com/en-ca>. Accessed: 2025.
- [19] SQIMWAY, “Nr frequency bands.” https://www.sqimway.com/nr_band.php, 2025. Accessed: 2025.
- [20] A. Radar, “Altos radar product page.” <https://www.altosradar.com/product>, 2023. Accessed: 2025.
- [21] “Rm520n series 5g module.” <https://www.quectel.com/product/5g-rm520n-series/>. Accessed: 2025.
- [22] Luxonis, “Oak-d pro: Stereo depth and ai vision camera.” <https://docs.luxonis.com/hardware/products/OAK-D%20Pro>, 2024. Accessed: 2025.
- [23] ROS-Perception, “image_transport_plugins.” https://github.com/ros-perception/image_transport_plugins, 2025. Online; accessed February 17, 2025.
- [24] J. Sturm, N. Engelhard, F. Endres, W. Burgard, and D. Cremers, “A benchmark for the evaluation of rgb-d slam systems,” in *Proc. of the International Conference on Intelligent Robot Systems (IROS)*, Oct. 2012.
- [25] Q.-Y. Zhou, J. Park, and V. Koltun, “Open3D: A modern library for 3D data processing,” *arXiv:1801.09847*, 2018.
- [26] University of Waterloo, “Eduroam.” [Online]. Available: <https://uwaterloo.ca/mechanical-mechatronics-engineering-information-technology/eduroam>. Accessed: 2025.
- [27] Rogers Communications Inc., “Rogers.” [Online]. Available: <https://www.rogers.com/>. Accessed: 2025.